

# Ink-jet printed semiconducting carbon nanotube ambipolar transistors and inverters with chemical doping technique using polyethyleneimine

Juhee Lee, Jinsu Yoon, Bongsik Choi, Dongil Lee, Dong Myong Kim, Dae Hwan Kim, Yang-Kyu Choi, and Sung-Jin Choi

Citation: *Appl. Phys. Lett.* **109**, 263103 (2016); doi: 10.1063/1.4973360

View online: <http://dx.doi.org/10.1063/1.4973360>

View Table of Contents: <http://aip.scitation.org/toc/apl/109/26>

Published by the [American Institute of Physics](#)

---

---

# Ink-jet printed semiconducting carbon nanotube ambipolar transistors and inverters with chemical doping technique using polyethyleneimine

Juhee Lee,<sup>1</sup> Jinsu Yoon,<sup>1</sup> Bongsik Choi,<sup>1</sup> Dongil Lee,<sup>2</sup> Dong Myong Kim,<sup>1</sup> Dae Hwan Kim,<sup>1</sup> Yang-Kyu Choi,<sup>2</sup> and Sung-Jin Choi<sup>1,a)</sup>

<sup>1</sup>*School of Electrical Engineering, Kookmin University, Seoul 02707, South Korea*

<sup>2</sup>*School of Electrical Engineering, KAIST, Daejeon 34141, South Korea*

(Received 31 August 2016; accepted 15 December 2016; published online 28 December 2016)

We demonstrate an ink-jet printed ambipolar transistor and inverter based on a semiconducting carbon nanotube (CNT) network as a channel by employing a solution-based chemical doping technique with an amine-rich polyethyleneimine (PEI) polymer. The PEI polymer has been reported as an efficient electron dopant and thus contributes to enhancing n-type conduction in CNT transistors. However, because of the presence of ambient oxygen and moisture and the hygroscopicity of the PEI polymer, their p-type conduction did not seem to be effectively reduced, resulting in rather ambipolar conduction. Therefore, we utilize a simple solution-based doping technique to convert p-type semiconducting CNT transistors into ambipolar transistors and fabricate the ambipolar CNT transistor by combining a cost-effective ink-jet printing technique and a simple spin-coating method. Finally, the electrical performance of the logic inverter consisting of identical two ambipolar CNT transistors is also evaluated and optimized by adjusting the concentration of PEI polymer.

Published by AIP Publishing. [<http://dx.doi.org/10.1063/1.4973360>]

Carbon nanotubes (CNTs) have attracted extensive interest for various electronic device applications because of high carrier mobility and current density,<sup>1,2</sup> extremely good mechanical strength,<sup>3</sup> excellent flexibility,<sup>4</sup> and solution-based processability at room temperature.<sup>5</sup> However, CNT-based electronic devices, i.e., CNT transistors, have typically exhibited only p-type characteristics under ambient conditions due to the strong adsorption of environmental oxygen and moisture.<sup>6–8</sup> These characteristics can limit the implementation of conventional concepts for logic circuits utilizing both unipolar p- and n-type transistors in the realization of complementary metal-oxide-semiconductor (CMOS). Thus, numerous methods have been proposed for the control and enhancement of n-type conduction in CNT transistors, including the use of (i) low workfunction metal for source/drain contacts,<sup>9–11</sup> (ii) atomic layer deposited (ALD) high- $\kappa$  oxide directly on the CNTs,<sup>12,13</sup> and (iii) chemical doping on either the contacts or the bulk of CNTs.<sup>14–16</sup> Additionally, without complex designs involving different n- and p-type unipolar transistors, ambipolar logic circuits (or CMOS-like logic circuits) consisting of identical ambipolar CNT transistors have recently received considerable attention for other methods of efficiently fabricating logic circuits.<sup>17–20</sup> Ambipolar transistors allow both electrons and holes to be injected and transported depending on the bias conditions in a single device. One of the significant advantages of using ambipolar transistors in logic circuits is ease of fabrication, as a single type of transistor can be used rather than spatially complicated patterned and designed unipolar p- and n-type transistors. In addition, it has been reported that ambipolar transistors offer more flexible circuit design options in terms of area, power, and speed. Hence, a variety of circuits

composed of ambipolar CNT transistors have been researched, verifying their practical feasibility.<sup>19,20</sup>

Herein, we present ink-jet printed ambipolar transistors based on a pre-separated, semiconducting CNT network as an active channel. Chemical doping with amine-rich polyethyleneimine (PEI) polymer was employed to functionalize the CNTs to produce and verify the ambipolar characteristics. PEI has previously been reported as an efficient electron dopant that exhibits stability in air, and thus, numerous reports have been predominantly focused on the implementation of n-type CNT transistors using PEI polymer.<sup>21–25</sup> However, it was frequently observed that, although the PEI polymer contributes to enhancing n-type conduction in CNT transistors by its electron-donating ability in amine-containing molecules, their p-type conduction did not seem to be effectively reduced even when a high concentration of PEI was utilized, resulting in rather ambipolar conduction with PEI doping. Therefore, using these properties, PEI-functionalized ambipolar CNT transistors acting as either n- or p-type transistors were fabricated by a combination of ink-jet printing and a simple spin-coating method in this work. Then, they were integrated to fabricate a logic inverter, consisting of two identical ambipolar PEI-doped CNT transistors, to explore their electrical performance. By adjusting the concentration of PEI polymer, we could evaluate and optimize the electrical performances of the logic inverters.

Fig. 1(a) presents a schematic illustration of ink-jet printed ambipolar transistors based on a pre-separated, semiconducting CNT network as a channel. The transistors were fabricated on 1.5 cm  $\times$  1.5 cm pieces of silicon wafer, highly p-doped as a common back-gate, with a thermally grown 55-nm-thick back-gate oxide (SiO<sub>2</sub>) layer. The substrate was first functionalized with a poly-L-lysine solution (0.1% w/v in H<sub>2</sub>O, Sigma Aldrich) to form an amine-terminated adhesion layer,<sup>26</sup> which acted as an effective adhesion layer for

<sup>a)</sup>Author to whom correspondence should be addressed. Electronic mail: sjchoiee@kookmin.ac.kr

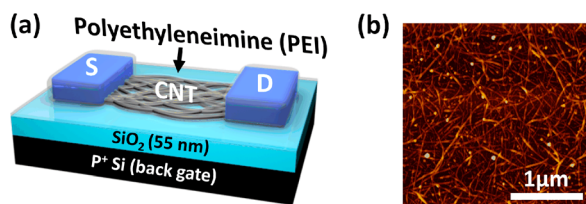


FIG. 1. (a) Schematic illustration of ink-jet printed semiconducting CNT ambipolar transistor. (b) AFM image ( $2.5 \mu\text{m} \times 2.5 \mu\text{m}$ , z-scale is 10 nm) of the CNT network channel created by the drop-coating method using 90% semiconducting CNT solution.

the deposition of CNTs. The substrate was then thoroughly rinsed with deionized (DI) water and isopropanol. The CNTs, as an active channel material, were deposited by immersion in purified 90% semiconductor-enriched CNT solution (NanoIntegris, Inc.) for several hours, followed by rinsing with DI water and isopropanol and drying with flowing nitrogen. The source and drain electrodes were inkjet-printed with silver (Ag) nanoparticle ink, followed by an annealing process at  $150^\circ\text{C}$ . Next, poly-4-vinylphenol (PVP) was inkjet-printed onto the surface to define the channel widths. The CNTs outside the channel region were then removed by an oxygen plasma-etching step to remove unwanted paths to electrically isolate the devices from one another. Afterward, the PVP was removed with acetone, isopropanol, and flowing nitrogen. We used the branched PEI polymer (average molecular weight: 800, Sigma Aldrich) to produce ambipolar characteristics in the CNT network transistors. First, a typical branched PEI polymer with the chemical formula of  $\text{H}(\text{NHCH}_2\text{CH}_2)_n\text{NH}_2$  was dissolved in methanol (0.01–50 vol. %) and then dispensed on the top surface of the devices using spin-coating at 500 rpm for 300 s. Next, the baking process was performed at  $65^\circ\text{C}$  to evaporate the methanol. Finally, the remaining PEI on the CNTs was removed by rinsing again with methanol, leaving nearly a monolayer of PEI irreversibly adsorbed on the CNTs.<sup>21–24</sup> From the previous reports, it was observed that roughly a monolayer of PEI was non-uniformly coated on the CNTs at the molecular scale, even though thorough rinsing with solvents was employed. Therefore, we speculated that the PEI layer becomes more uniform and continuous, and denser with increasing the PEI concentration ( $n_{\text{PEI}}$ ). Further in-depth investigation using transmission electron microscopy remains for characterizing the PEI layer on the CNTs. Most of the layers in the devices were fabricated by a cost-effective ink-jet printing technique and simple

spin-coating method without the use of physical masks and photolithography. Strictly speaking, the CNT networks were not printed; instead, a solution-based drop-coating process was used to deposit the CNT networks. Although the ink-jet printing process is a more cost-effective approach in terms of CNT usage than the drop-coating process, it was observed that the device yield and uniformity from the drop-coating method were superior to the results of the ink-jet printing process.<sup>27</sup> Fig. 1(b) shows an atomic force microscopy (AFM) image of a typical CNT network constructed from the 90% semiconducting CNT solution. The CNTs were well percolated, and the density of the CNT networks was estimated to be approximately  $75\text{--}81 \text{ CNTs}/\mu\text{m}^2$ .

Fig. 2(a) shows the drastically altered electrical characteristics of CNT transistors after PEI adsorption. The transfer curves, i.e., drain current-gate voltage,  $I_{\text{DS}}\text{--}V_{\text{GS}}$ , were measured at a drain to source voltage ( $V_{\text{DS}}$ ) of  $-0.5 \text{ V}$  under ambient conditions. Prior to PEI adsorption, the as-fabricated CNT transistor exhibits p-type FET characteristics due to the adsorption of environmental oxygen and moisture. On the other hand, the transfer curves were significantly altered by increasing the  $n_{\text{PEI}}$ . Even at a small  $n_{\text{PEI}}$  of 0.01 vol. %, the n-type current at positive  $V_{\text{GS}}$  values began to show a clear increase. Furthermore, as the  $n_{\text{PEI}}$  increased up to 50 vol. %, the conduction type significantly changed from the initial p-type to strong ambipolar conduction, rather than unipolar n-type conduction. These results are highly reproducible with 30 independent CNT transistors. Moreover, extensive rinsing of the devices cannot remove the PEI completely from the CNTs, resulting in irreversible changes in the electrical characteristics.

It is well known that PEI has the electron-donating ability of amine groups in the polymer and contains one of the highest densities of amine groups among all polymers.<sup>21</sup> The amine groups in the PEI polymer were found to be sufficient to cause significant changes in the electrical conductance of CNTs. The strong physisorption and weak chemisorption of the amine molecules on the CNTs causes a shift of the Fermi level toward the conduction band by electron donation.<sup>28</sup> Therefore, it has been predominantly reported that the high density of electron-donating amine functionalities in PEI results in significant unipolar n-doping to a point where the adverse effect of p-doping due to adsorption of the environmental oxygen and moisture is reduced. However, in our case, it should be noted that a significant p-type current was still observed at negative  $V_{\text{GS}}$  values even when a high

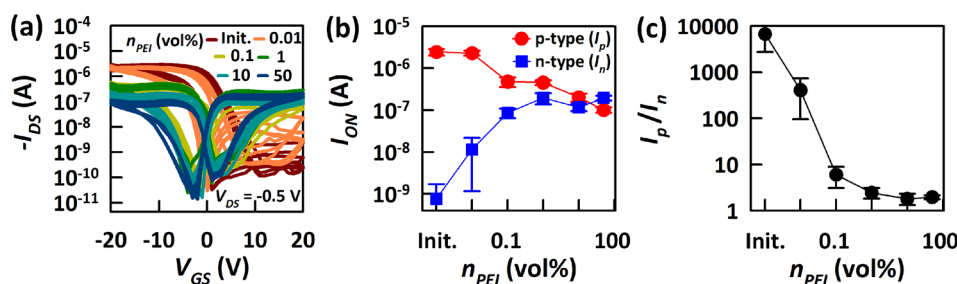


FIG. 2. (a) Transfer characteristics ( $I_{\text{DS}}\text{--}V_{\text{GS}}$ ) of a total of 30 CNT transistors using various  $n_{\text{PEI}}$  values with channel lengths ( $L = 250 \mu\text{m}$  and  $350 \mu\text{m}$ ) and the same width ( $W = 400 \mu\text{m}$ ). The “Init.” in the graph shows the data extracted from the CNT transistor with no PEI doping (i.e., bare CNT network). (b) Plot of extracted  $I_{\text{ON}}$  and (c) ratio of  $I_{\text{ON}}$  at p- and n-type conduction ( $I_{\text{p}}/I_{\text{n}}$  or  $I_{\text{n}}/I_{\text{p}}$ ) in PEI-doped CNT transistors with varying  $n_{\text{PEI}}$ .

$n_{PEI}$  of 50 vol. % was employed. This result is attributed to the measurement under ambient conditions where oxygen and moisture co-existed.<sup>29</sup> Because the PEI polymer most likely absorbs those molecules, i.e., exhibiting hygroscopicity,<sup>29–32</sup> the spontaneous electron transfer from CNTs to those molecules through the intermediate of the redox reaction still occurs, resulting in strong ambipolar conduction.<sup>33,34</sup> The further increase of  $n_{PEI}$  leads to degradation of the current on/off ratio because a continuous PEI layer on the device was formed with increasing  $n_{PEI}$ , resulting in reduced gate modulation due to the charges accumulated in the PEI polymer. Large and unwanted hysteresis behaviors in the transfer curves can be seen, but it can be further improved by the encapsulation of hydrophobic polymers or dielectrics to close the exposed CNT network.

Fig. 2(b) plots the extracted on-state current  $s(I_{ON})$  for p- and n-type conduction, i.e.,  $I_p$  and  $I_n$ , respectively, in PEI-doped CNT transistors with varying  $n_{PEI}$ , measured at  $V_{GS}$  of  $-20$  V and  $20$  V, respectively. Below an  $n_{PEI}$  of 1 vol. %,  $I_n$  was significantly enhanced, and in contrast,  $I_p$  was slightly decreased. The changes in  $I_n$  and  $I_p$  by PEI adsorption began to be saturated above an  $n_{PEI}$  of 1 vol. %, resulting in a well-balanced ratio between them, as shown in Fig. 2(c). The best ambipolarity was obtained at an  $n_{PEI}$  of 10 vol. %, with the smallest ratio of  $I_p/I_n$  (or  $I_n/I_p$ ). It is worth noting that the degree of balance in n- and p-type conduction can be controlled simply by the selection of  $n_{PEI}$ . The hole and electron mobilities ( $\mu_h$  and  $\mu_e$ ) for p- and n-type conduction were calculated to be  $3.9 \pm 3.6$  cm<sup>2</sup>/V·s and  $1.2 \pm 0.8$  cm<sup>2</sup>/V·s, respectively, from 25 independent CNT transistors possessing different channel lengths ( $L = 250$   $\mu$ m and  $350$   $\mu$ m) and the same width ( $W = 400$   $\mu$ m). The highest  $\mu_h$  and  $\mu_e$  values we obtained were  $15$  cm<sup>2</sup>/V·s and  $3$  cm<sup>2</sup>/V·s, respectively, using a cylindrical model to calculate the gate capacitance.

To demonstrate the utility of the ambipolar PEI-doped CNT transistors, inverters were produced by combining two identical ambipolar CNT transistors constructed using various  $n_{PEI}$  values ranging from 0 to 50 vol. %. Fig. 3(a) presents the voltage transfer characteristics, i.e., output voltage vs input voltage,  $V_{IN}$  vs  $V_{OUT}$ , of the inverters, measured at a supply voltage ( $V_{DD}$ ) of 20 V. Both hole and electron carriers of ambipolar CNT transistors in this inverter can be transported, depending on the  $V_{GS}$  values. The conduction and valence bands of the CNTs are upshifted to transport hole carriers with a negative  $V_{GS}$  value, while the conduction and valence bands of the CNTs are downshifted to transport electron carriers with a positive  $V_{GS}$  value. In this inverter

configuration, the  $V_{DD}$  and ground terminals are interchangeable due to the device symmetry. At  $n_{PEI}$  values of 0 vol. % and 0.01 vol. %, the inverter did not show the appropriate switching behavior, which is attributed to the insufficient n-type current in the bottom ambipolar transistors. As  $n_{PEI}$  was increased to 0.1 vol. %, however, the inverter showed the proper switching of  $V_{OUT}$  from high to low values as  $V_{IN}$  was swept from low to high values. Further increases of  $n_{PEI}$  showed gradually enhanced performance in the inverters because the n- and p-type currents became better balanced. However,  $V_{OUT}$  was not constant for both high and low values of  $V_{IN}$ , as  $V_{OUT}$  increases slightly with  $V_{IN}$ . This common feature among this type of inverter arises because one of the two ambipolar transistors is not completely turned off while the other ambipolar transistor is turned on.<sup>35</sup> The voltage gain defined as  $|dV_{OUT}/dV_{IN}|$  and the noise margin (NM) were also extracted from voltage transfer characteristics, as shown in Figs. 3(b) and 3(c), respectively. The inset in Fig. 3(c) shows the NM criteria extracted from the voltage transfer curve with an  $n_{PEI}$  of 10 vol. %. NM is defined as the sum of the low-state noise margin ( $NM_L = V_{IL} - V_{OL}$ ) and the high-state noise margin ( $NM_H = V_{OH} - V_{IH}$ ). The best inverter performance in terms of the gain and NM can be obtained at an  $n_{PEI}$  of 10 vol. %, where the n- and p-type currents were the best balanced. At an  $n_{PEI}$  of 50 vol. %, the inverter performance was slightly decreased, as the n-type current was higher than the p-type current.

As a series evaluation of the ambipolar inverter, the performances of three different types of inverters, namely, the pseudo p-type MOS (PMOS) inverter consisting of two initial p-type CNT transistors, a CMOS inverter consisting of an initial p-type CNT transistor as the p-type and a PEI-doped CNT transistor as the n-type, and an ambipolar inverter consisting of two PEI-doped CNT transistors, are shown in Fig. 4. The circuit diagrams for each inverter were shown in the inset figure. We only considered the  $V_{IN}$  range from 0 to  $V_{DD}$  for practical uses. Fig. 4(a) shows the characteristics of the pseudo PMOS inverter, and the bottom initial p-type CNT transistor always operates in the saturation region. Therefore, the pull-up operation cannot properly occur, compared to the pull-down operation, so the maximum  $V_{OUT}$  cannot reach to the  $V_{DD}$  value. The maximum voltage gain is only approximately 1 at a  $V_{DD}$  of 10 V. Figs. 4(b) and 4(c) present the characteristics of the CMOS inverter and ambipolar inverter, respectively. We used the  $n_{PEI}$  of 50 vol. % for the top transistor in the CMOS inverter because the PEI-doped CNT transistor with an  $n_{PEI}$  of 50 vol. % showed the highest n-type current among various  $n_{PEI}$  values. Moreover, an  $n_{PEI}$  of 10 vol. % was used for two PEI-doped CNT transistors in the ambipolar inverter, due to the most well-balanced properties between the p- and n-type currents. Within the  $V_{IN}$  range from 0 to  $V_{DD}$ , it was observed that the  $V_{OUT}$  cannot be lowered, i.e., did not show the proper pull-down operation because the threshold voltage ( $V_T$ ) between the initial p-type CNT transistor ( $-1.8$ ) and PEI-doped CNT transistor ( $2.1$ ) was significantly mismatched. This result indicates that the additional  $V_T$  adjustment is required to match the  $V_T$  between the pull-up and pull-down transistors. However, for the pull-up operation, the maximum  $V_{OUT}$  value nearly reached the  $V_{DD}$  value due to the high p-type current in an initial p-type CNT transistor.

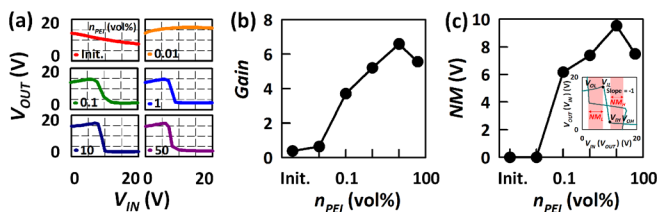


FIG. 3. (a) Voltage transfer characteristics of CMOS-like inverter consisting of two identical ambipolar PEI-doped CNT transistors with varying  $n_{PEI}$  at the  $V_{DD}$  of 20 V. (b) Voltage gain ( $|dV_{OUT}/dV_{IN}|$ ) and (c) NM obtained from voltage transfer curves with varying  $n_{PEI}$ . Inset is a plot of NM criteria extracted from the voltage transfer curve with  $n_{PEI}$  of 10 vol. %.

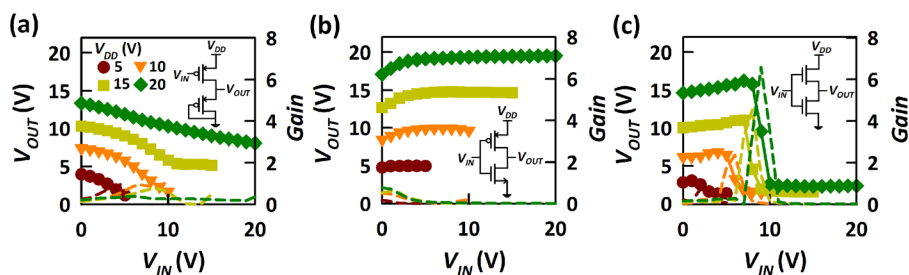


FIG. 4. Inverter performance of three different types, namely, (a) the pseudo PMOS inverter consisting of two initial p-type CNT transistors, (b) the CMOS inverter consisting of an initial p-type CNT transistor as the p-type and a PEI-doped CNT transistor as the n-type, and (c) the ambipolar inverter consisting of two PEI-doped CNT transistors at different  $V_{DD}$ .

On the other hand, the ambipolar PEI-doped CNT transistors in the ambipolar inverter can operate as pull-up and pull-down transistors, exhibiting proper logic functionality. The high voltage gain and NM were recorded as approximately 7 and 10, respectively, at a  $V_{DD}$  of 20 V.

In conclusion, we demonstrate ink-jet printed ambipolar transistors and inverters based on a semiconducting CNT network as a channel. The CNTs were functionalized by amine-rich PEI polymer as a chemical doping technique to produce the ambipolar characteristics. We confirm that the simple spin coating of PEI polymer facilitates ambipolar transport, rather than unipolar n-type transport, in CNT transistors under ambient conditions. In addition, we could easily optimize the performance of the logic inverters by adjusting  $n_{PEI}$ . Although further improvement of the device performance seems to be necessary, through the use of ohmic Pd source/drain electrodes and thinner/high-k gate dielectrics, the concept presented here will play an important role in various future CNT electronics.

This work was supported by the National Research Foundation (NRF) of Korea under Grant No. 2016R1A2B4011366 and partially supported by the NRF of Korea under Grant No. 2016R1A5A1012966, and partially supported by the Future Semiconductor Device Technology Development Program (10067739) funded by MOTIE (Ministry of Trade, Industry & Energy) and KSRC (Korea Semiconductor Research Consortium).

<sup>1</sup>T. Dürkop, S. A. Getty, E. Cobas, and M. S. Fuhrer, *Nano Lett.* **4**, 35 (2004).

<sup>2</sup>Z. Yao, C. L. Kane, C. M. Marcus, and C. Dekker, *Phys. Rev. Lett.* **84**, 2941 (2000).

<sup>3</sup>D. Bozovic, M. Bockrath, J. H. Hafner, C. M. Lieber, H. Park, and M. Tinkham, *Phys. Rev. B* **67**, 033407 (2003).

<sup>4</sup>E. Artukovic, M. Kaempgen, D. S. Hecht, S. Roth, and G. Grüner, *Nano Lett.* **5**, 757 (2005).

<sup>5</sup>D.-M. Sun, C. Liu, W.-C. Ren, and H.-M. Cheng, *Small* **9**, 1188 (2013).

<sup>6</sup>C. Biswas and Y. H. Lee, *Adv. Funct. Mater.* **21**, 3806 (2011).

<sup>7</sup>N. Moriyama, Y. Ohno, T. Kitamura, S. Kishimoto, and T. Mizutani, *Nanotechnology* **21**, 165201 (2010).

<sup>8</sup>W. Kim, A. Javey, O. Vermesh, Q. Wang, Y. Li, and H. Dai, *Nano Lett.* **3**, 193 (2003).

<sup>9</sup>Y. Noshu, Y. Ohno, S. Kishimoto, and T. Mizutani, *Nanotechnology* **17**, 3412 (2006).

<sup>10</sup>Y. Noshu, Y. Ohno, S. Kishimoto, and T. Mizutani, *Appl. Phys. Lett.* **86**, 073105 (2005).

<sup>11</sup>Z. Zhang, X. Liang, S. Wang, K. Yao, Y. Hu, Y. Zhu, Q. Chen, W. Zhou, Y. Li, Y. Yao, J. Zhang, and L.-M. Peng, *Nano Lett.* **7**, 3603 (2007).

<sup>12</sup>J. Zhang, C. Wang, Y. Fu, Y. Che, and C. Zhou, *ACS Nano* **5**, 3284 (2011).

<sup>13</sup>N. Moriyama, Y. Ohno, K. Suzuki, S. Kishimoto, and T. Mizutani, *Appl. Phys. Express* **3**, 105102 (2010).

<sup>14</sup>C. Zhou, J. Kong, E. Yenilmez, and H. Dai, *Science* **290**, 1552 (2000).

<sup>15</sup>S. Y. Lee, S. W. Lee, S. M. Kim, W. J. Yu, Y. W. Jo, and Y. H. Lee, *ACS Nano* **5**, 2369 (2011).

<sup>16</sup>H. Wang, P. Wei, Y. Li, J. Han, H. R. Lee, B. D. Naab, N. Liu, C. Wang, E. Adjanto, B. C.-K. Tee, S. Morishita, Q. Li, Y. Gao, Y. Cui, and Z. Bao, *Proc. Natl. Acad. Sci. U. S. A.* **111**, 4776 (2014).

<sup>17</sup>S. Z. Bisri, C. Piliago, J. Gao, and M. A. Loi, *Adv. Mater.* **26**, 1176 (2014).

<sup>18</sup>K. Jabeur, I. O'Connor, and N. Yakymets, *Microelectron. J.* **44**, 1316 (2013).

<sup>19</sup>M. H. Ben Jamaa, D. Atienza, Y. Leblebici, and G. De Micheli, in 45th ACM Design Automation Conference, DAC 2008 (2008).

<sup>20</sup>M. H. Ben Jamaa, K. Mohanram, and G. De Micheli, in Design, Automation, and Test in Europe Conference and Exhibition (2009).

<sup>21</sup>M. Shim, A. Javey, N. W. Shi Kam, and H. Dai, *J. Am. Chem. Soc.* **123**, 11512 (2001).

<sup>22</sup>Z. Li, V. Saini, E. Dervishi, V. P. Kunets, J. Zhang, Y. Xu, A. R. Biris, G. J. Salamo, and A. S. Biris, *Appl. Phys. Lett.* **96**, 033110 (2010).

<sup>23</sup>K. Bradley, J. C. P. Gabriel, A. Star, and G. Grüner, *Appl. Phys. Lett.* **83**, 3821 (2003).

<sup>24</sup>Y. Duan, J. L. Juhala, B. W. Griffith, and W. Xue, *Microelectron. Eng.* **103**, 18 (2013).

<sup>25</sup>J. Park, J. Yoon, G.-T. Kim, and J. S. Ha, *Nanotechnology* **22**, 385302 (2011).

<sup>26</sup>C. Wang, J.-C. Chien, K. Takei, T. Takahashi, J. Nah, A. M. Niknejad, and A. Javey, *Nano Lett.* **12**, 1527 (2012).

<sup>27</sup>L. Cai, S. Zhang, J. Miao, Z. Yu, and C. Wang, *Adv. Funct. Mater.* **25**, 5698 (2015).

<sup>28</sup>J. Kong and H. Dai, *J. Phys. Chem. B* **105**, 2890 (2001).

<sup>29</sup>T. Yasunishi, S. Kishimoto, and Y. Ohno, *Jpn. J. Appl. Phys.* **53**, 05FD01 (2014).

<sup>30</sup>B. A. E. Courtright and S. A. Jenekhe, *ACS Appl. Mater. Interfaces* **7**, 26167 (2015).

<sup>31</sup>B. Serban, A. K. S. Kumar, S. Costea, M. Mihaila, O. Buiu, M. Brezeanu, N. Varachiu, and C. Cobianu, "Polymer-amino carbon nanotube nanocomposites for surface acoustic wave CO<sub>2</sub> detection," *Roman. J. Inf. Sci. Technol.* **12**, 376–382 (2009).

<sup>32</sup>D. Schoolmann, O. Trinquet, and J.-C. Lassègues, *Electrochim. Acta* **37**, 1619 (1992).

<sup>33</sup>C. M. Aguirre, P. L. Levesque, M. Paillet, F. Lapointe, B. C. St-Antoine, P. Desjardin, and R. Martel, *Adv. Mater.* **21**, 3087 (2009).

<sup>34</sup>V. Chakrapani, J. C. Angus, A. B. Anderson, and S. D. Wolter, *Science* **318**, 1424 (2007).

<sup>35</sup>B. Kim, S. Jang, M. L. Geier, P. L. Prabhurashi, M. C. Hersam, and A. Dodabalapur, *Appl. Phys. Lett.* **104**, 062101 (2014).